PERGAMON

International Journal of Solids and Structures 39 (2002) 1791–1802

INTERNATIONAL JOURNAL OF SOLIDS and STRUCTURES

www.elsevier.com/locate/ijsolstr

Instability of a compressed elastic film on a viscous layer

R. Huang [a,b,*], Z. Suo [b,c]

[a] *Department of Civil and Environmental Engineering, Princeton University, Princeton, NJ 08544, USA*
[b] *Princeton Materials Institute, Princeton University, Princeton, NJ 08544, USA*
[c] *Department of Mechanical and Aerospace Engineering, Princeton University, Princeton, NJ 08544, USA*

Received 8 August 2001; received in revised form 13 November 2001

Abstract

A flat, compressed elastic film on a viscous layer is unstable. The film can form wrinkles to reduce the elastic energy. A linear perturbation analysis is performed to determine the critical wave number and the growth rate of the unstable modes. While the viscous layer has no effect on the critical wave number, its viscosity and thickness set the time scale for the growth of the perturbations. The fastest growing wave number and the corresponding growth rate are obtained as functions of the compressive strain and the thickness ratio between the viscous layer and the elastic film. The present analysis is valid for all thickness range of the viscous layer. In the limits of infinitely thick and thin viscous layers, the results reduce to those obtained in the previous studies. © 2002 Elsevier Science Ltd. All rights reserved.

Keywords: Thin film; Instability; Viscous flow; Linear perturbation analysis

1. Introduction

In many film/substrate systems, the film is in a state of biaxial compression. Some remarkable instability and failure modes of such systems have been observed. A film with a large unbonded flaw can buckle away from the substrate under the compressive stress and the buckle then causes the flaw to spread if the compressive stress is large enough (Evans and Hutchinson, 1984; Hutchinson and Suo, 1992). For an oxide scale on an aluminum-containing alloy, the interface initially remains bonded, but the oxidation-induced compressive stress causes wrinkling at high temperatures (Suo, 1995; Tolpygo and Clarke, 1998a,b). The instability of the thermally grown oxide controls the durability of thermal barrier coatings (Evans et al., 2001; Mumm et al., 2001). It has also been observed that a thin film of gold deposited on the surface of an elastomer can form aligned buckles to relieve the compressive stress caused by the shrinkage of the substrate on cooling (Bowden et al., 1998; Huck et al., 2000).

In this paper, we study the instability of a compressed elastic film on a viscous layer. The system was formed by transferring a compressively strained heteroepitaxial SiGe film to a Si substrate coated with a

* Corresponding author. Address: Department of Civil and Environmental Engineering, Princeton University, Princeton, NJ 08544, USA. Tel.: +1-609-258-1619; fax: +1-609-258-1270.
E-mail address: ruihuang@princeton.edu (R. Huang).

0020-7683/02/$ - see front matter
PII: S0020-7683(02)00011-2

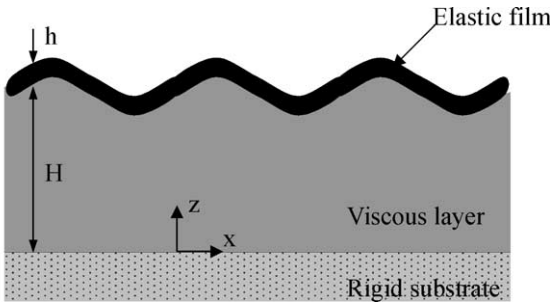

Fig. 1. A wrinkled elastic film on a viscous layer.

layer of glass (Hobart et al., 2000; Yin et al., 2001). Upon annealing above the glass transition temperature, the glass flows like a viscous liquid and the SiGe film forms wrinkles, as shown in Fig. 1. The instability was previously studied by Sridhar et al. (2001), in which the shear traction along the interface was assumed to be zero and the displacement parallel to the interface was ignored. In this paper, we show that such simplifications are incorrect when the thickness of the viscous layer is small. Recently, we studied the wrinkling process of this system by using the lubrication theory for the viscous flow and the non-linear plate theory for the elastic film (Huang and Suo, 2002). The lubrication theory enabled us to do simulations beyond the linear stability analysis. However, the assumption made in the lubrication theory requires that the thickness of the viscous layer be small compared to the wavelength, and thus the analysis is not valid when the thickness of the viscous layer is large. This paper presents a more rigorous analysis in that it is valid for all thickness range of the viscous layer. In the limits of infinitely thick and thin viscous layers, the results from the present analysis reduce to those from the previous studies.

The plan of this paper is as follows. In Section 2, we first consider the linear perturbations of the viscous flow and the elastic deformation separately, and then couple them to study the stability of the perturbations. In Section 3, we discuss the results and compare with the previous studies. Section 4 gives the concluding remarks.

2. Formulation and solution

As shown in Fig. 1, we consider an elastic film on a viscous layer, which in turn lies on a rigid substrate. The viscous flow and the elastic deformation are coupled through the interface, where the displacements and the tractions are assumed to be continuous.

2.1. Flow in a viscous layer

The flow is assumed to be slow such that the inertia can be neglected. The equation of motion reduces to the equilibrium equation, i.e.,

$$\sigma_{ij,j} = 0, \tag{1}$$

where σ_{ij} is the stress tensor. The material of the layer is assumed to be linear viscous. Thus the stress components relate to the velocities by

$$\sigma_{ij} = \eta(v_{i,j} + v_{j,i}) - p\delta_{ij}, \tag{2}$$

where η is the viscosity, v_i is the velocity, and p is the pressure. The viscous layer is also assumed to be incompressible, so that

$$v_{i,i} = 0, \tag{3}$$

and

$$p = -\tfrac{1}{3}\sigma_{ii}. \tag{4}$$

Under the above assumptions, the flow is referred to as the "Stokes flow" or the "creeping flow".

A trivial solution to Eqs. (1)–(4) corresponds to an infinite viscous layer on a rigid substrate with constant thickness and free top surface. Now consider a perturbation along the surface to the trivial solution. Since the viscous layer is isotropic in the plane of its surface, the wave vector of the perturbation in any direction is equivalent. We choose the direction to coincide with the x-direction of the coordinate, as shown in Fig. 1. Consequently, the perturbed viscous layer is in a state of plane strain deformation in the x–z plane, i.e., $v_x = v_x(x,z,t)$, $v_z = v_z(x,z,t)$, and $v_y = 0$. Because the surface of the viscous layer is infinite, the perturbed field has the translational symmetry along the surface such that the location of the origin of the x-coordinate is arbitrary. To simplify writing, we choose the origin such that the tractions at the surface take the form:

$$\sigma_{zz}(z = H) = q_0(t)\sin(kx), \tag{5}$$

$$\sigma_{zx}(z = H) = \tau_0(t)\cos(kx), \tag{6}$$

where H is the thickness of the viscous layer, k is the wave number of the perturbation, $q_0(t)$ and $\tau_0(t)$ are the time-dependent amplitudes of the surface tractions. The velocities at the bottom of the viscous layer are set to be zero. Under these boundary conditions, a set of exact solutions to Eqs. (1)–(4) is obtained in Appendix A. Of relevance to the present study are the velocities at the top surface, taking the form:

$$v_z(z = H) = \bar{v}_z(t)\sin(kx), \tag{7}$$

$$v_x(z = H) = \bar{v}_x(t)\cos(kx). \tag{8}$$

The amplitudes of velocities, $\bar{v}_z(t)$ and $\bar{v}_x(t)$, are linearly related to the amplitudes of the surface tractions. Dimensional considerations dictate that

$$\bar{v}_z(t) = \frac{1}{2\eta k}(\gamma_{11}q_0(t) + \gamma_{12}\tau_0(t)), \tag{9}$$

$$\bar{v}_x(t) = \frac{1}{2\eta k}(\gamma_{21}q_0(t) + \gamma_{22}\tau_0(t)), \tag{10}$$

where the dimensionless coefficients are (see Appendix A for details)

$$\gamma_{11} = \frac{1}{2}\frac{\sinh(2kH) - 2kH}{(kH)^2 + \cosh^2(kH)}, \tag{11}$$

$$\gamma_{22} = \frac{1}{2}\frac{\sinh(2kH) + 2kH}{(kH)^2 + \cosh^2(kH)}, \tag{12}$$

$$\gamma_{12} = \gamma_{21} = \frac{(kH)^2}{(kH)^2 + \cosh^2(kH)}. \tag{13}$$

We can compare the present solution with three previous studies. In Sridhar et al. (2001), the shear traction at the surface (τ_0) was assumed to be zero and the shear velocity at the surface ($\bar{v}_x$) was ignored. However, from the above exact solution, both the shear traction and the shear velocity are not zero, and even when the amplitude of shear traction τ_0 is zero the shear velocity amplitude $\bar{v}_x$ is not zero due to the non-uniform normal traction (Eq. 10). When the thickness of the viscous layer is large compared to the

wavelength ($kH \gg 1$), we have $\gamma_{21} \ll \gamma_{11}$ and thus $\bar{v}_x \ll \bar{v}_z$ if $\tau_0 = 0$. In the limit of an infinitely thick viscous layer ($kH \to \infty$), $\gamma_{21} \to 0$ and $\bar{v}_x \to 0$ if $\tau_0 = 0$. Therefore, the analysis in Sridhar et al. (2001) is approximately correct for a thick viscous layer and approaches to the exact solution as the thickness approaches infinity.

Recently we derived a set of equations that relate the velocities at the surface of a viscous layer to the pressure and the shear tractions at the surface by using the lubrication theory (Huang and Suo, 2002). The lubrication theory assumes that the thickness of the viscous layer is small compared to the characteristic lengths in the lateral directions, i.e., $kH \ll 1$. Here we show that the above exact solution reduces to the solution from the lubrication theory in the limit of a thin viscous layer. Retaining only the leading order of kH in Eqs. (11)–(13), we have $\gamma_{11} = (2/3)(kH)^3$, $\gamma_{22} = 2kH$, and $\gamma_{12} = \gamma_{21} = (kH)^2$. Thus, Eqs. (9) and (10) become

$$\bar{v}_z(t) = \frac{H^3}{3\eta} k^2 q_0(t) + \frac{H^2}{2\eta} k\tau_0(t), \tag{14}$$

$$\bar{v}_x(t) = \frac{H^2}{2\eta} k q_0(t) + \frac{H}{\eta} \tau_0(t), \tag{15}$$

which are equivalent to those obtained from the lubrication theory in our previous study. Comparing Eqs. (14) and (15) with Eqs. (9) and (10), the difference between the two solutions is the dimensionless coefficients, γ_{11}, γ_{22}, γ_{12}, and γ_{21}, and the solution from the lubrication theory is correct only when $kH \ll 1$.

Eqs. (14) and (15) can be further reduced by keeping only the first order of H when the thickness of the viscous layer approaches zero ($H \to 0$), and we have $\bar{v}_z \to 0$ and $\bar{v}_x = (H/\eta)\tau_0$, which is the solution from the shear lag model (Freund and Nix, unpublished; Yin et al., 2001). When the viscous layer is very thin, the normal velocity $\bar{v}_z$ is negligible and the surface of the viscous layer remains flat.

While the thickness of the viscous layer is either assumed to be small or limited to large in the previous studies, there is no assumption about the thickness in the present study. As shown above, the present solution is exact and can be easily reduced to the previous solutions under certain conditions.

2.2. Deformation in an elastic film

Next we turn our attention to the elastic film. The plate theory has been used to model the elastic deformation in thin films for many years. Although the non-linear plate theory is generally required for problems involving large deflections compared to the thickness of the film (Hutchinson and Suo, 1992; Finot and Suresh, 1996; Huang and Suo, 2002), it is sufficient to use the classical linear plate theory for linear perturbation analyses (Sridhar et al., 2001), as in the present study. The film under consideration is subject to the in-plane membrane force (N), the normal (q) and the shear tractions (τ) at the bottom surface, as shown in Fig. 1. Under the plane strain conditions, the equilibrium equations of the linear plate theory (Timoshenko and Woinowsky-Krieger, 1987) leads to

$$q = -\frac{Eh^3}{12(1-\nu^2)} \frac{\partial^4 w}{\partial x^4} + N \frac{\partial^2 w}{\partial x^2} + \tau \frac{\partial w}{\partial x}, \tag{16}$$

$$\tau = \frac{\partial N}{\partial x}, \tag{17}$$

where w is the deflection of the film, h is the thickness, E is Young's modulus, and ν is Poisson's ratio. The membrane force N relates to the in-plane displacement in the x direction, u, by Hooke's law. Considering that the film is initially compressed with a biaxial strain ε_0 and the in-plane displacement is set to be zero at the initial state, we obtain that

$$N = \frac{E\varepsilon_0 h}{1-\nu} + \frac{Eh}{1-\nu^2} \frac{\partial u}{\partial x}. \tag{18}$$

Perturb the displacements as

$$w(x,t) = A(t)\sin(kx), \tag{19}$$

$$u(x,t) = B(t)\cos(kx), \tag{20}$$

where A and B are small amplitudes. Substituting Eqs. (19) and (20) into Eqs. (18), (17) and (16), and keeping only the first order terms in A and B, we obtain that

$$N = \frac{E\varepsilon_0 h}{1-\nu} - \frac{Ehk}{1-\nu^2}B\sin(kx), \tag{21}$$

$$\tau = -\frac{Ehk^2}{1-\nu^2}B\cos(kx), \tag{22}$$

$$q = \frac{Ehk^2}{12(1-\nu^2)}(-12(1+\nu)\varepsilon_0 - (kh)^2)A\sin(kx). \tag{23}$$

Therefore, within the range of small perturbations, the surface tractions, τ and q, are linearly related to the in-plane displacement u and the deflection w, respectively.

2.3. Coupled viscous flow and elastic deformation

Now we put together the viscous layer and the elastic film and assume that the tractions and displacements are continuous across the interface. Given the displacements of the elastic film in Eqs. (19) and (20), the amplitudes of the velocities at the surface of the viscous layer are

$$\bar{v}_z(t) = \frac{\mathrm{d}A}{\mathrm{d}t} \quad \text{and} \quad \bar{v}_x(t) = \frac{\mathrm{d}B}{\mathrm{d}t}. \tag{24}$$

Comparing the surface tractions of the viscous layer in Eqs. (5) and (6) with the tractions at the bottom of the elastic film in Eqs. (22) and (23), we obtain that

$$\tau_0(t) = -\frac{Ehk^2}{1-\nu^2}B(t), \tag{25}$$

$$q_0(t) = \frac{Ehk^2}{12(1-\nu^2)}(-12(1+\nu)\varepsilon_0 - (kh)^2)A(t). \tag{26}$$

Substituting Eqs. (24)–(26) into Eqs. (9) and (10), we obtain that

$$\frac{\mathrm{d}A}{\mathrm{d}t} = \alpha A - \frac{\gamma_{12}}{\gamma_{22}}\beta B, \tag{27}$$

$$\frac{\mathrm{d}B}{\mathrm{d}t} = \frac{\gamma_{21}}{\gamma_{11}}\alpha A - \beta B, \tag{28}$$

where

$$\alpha = \frac{Ekh}{24\eta(1-\nu^2)}(-12\varepsilon_0(1+\nu) - (kh)^2)\gamma_{11}, \tag{29}$$

$$\beta = \frac{Ekh}{2\eta(1-\nu^2)}\gamma_{22}, \tag{30}$$

and γ_{11}, γ_{22}, and $\gamma_{12} = \gamma_{21}$ are functions of kH as defined in Eqs. (11)–(13).

Eqs. (27) and (28) are two coupled linear ordinary differential equations. The solution takes the form

$$A(t) = A_1 \exp(s_1 t) + A_2 \exp(s_2 t), \tag{31}$$

$$B(t) = B_1 \exp(s_1 t) + B_2 \exp(s_2 t), \tag{32}$$

where s_1 and s_2 are two eigenvalues of Eqs. (27) and (28):

$$s_1 = \frac{1}{2}\left((\alpha-\beta) + \sqrt{(\alpha-\beta)^2 + 4\alpha\beta\left(1 - \frac{\gamma_{12}^2}{\gamma_{11}\gamma_{22}}\right)}\right), \tag{33}$$

$$s_2 = \frac{1}{2}\left((\alpha-\beta) - \sqrt{(\alpha-\beta)^2 + 4\alpha\beta\left(1 - \frac{\gamma_{12}^2}{\gamma_{11}\gamma_{22}}\right)}\right), \tag{34}$$

and the corresponding eigenvectors give that

$$\frac{B_1}{A_1} = \frac{(\alpha - s_1)\gamma_{22}}{\beta\gamma_{12}}, \qquad \frac{B_2}{A_2} = \frac{(\alpha - s_2)\gamma_{22}}{\beta\gamma_{12}}. \tag{35}$$

Let the initial amplitudes be $A(0) = A_0$ and $B(0) = B_0$, so that

$$A_1 = \frac{\alpha - s_2}{s_1 - s_2}A_0 - \frac{\beta\gamma_{12}}{(s_1 - s_2)\gamma_{22}}B_0, \tag{36}$$

$$A_2 = \frac{\alpha - s_1}{s_2 - s_1}A_0 - \frac{\beta\gamma_{12}}{(s_2 - s_1)\gamma_{22}}B_0, \tag{37}$$

and B_1, B_2 can be obtained from Eq. (35).

3. Analyses and discussion

The amplitudes of the perturbations in displacements are obtained in Eqs. (31) and (32) as functions of time. The stability of the unperturbed, flat film depends on the rates, s_1 and s_2, given in Eqs. (33) and (34). It can be shown that, for any wave number k, s_2 is negative. Consequently, the s_2-mode in Eqs. (31) and (32) always decays exponentially with time. For the s_1-mode, however, there exists a critical wave number:

$$k_c h = \sqrt{-12\varepsilon_0(1+\nu)}. \tag{38}$$

When $k > k_c$, $s_1 < 0$ and the perturbations decay. When $k < k_c$, $s_1 > 0$ and the perturbations grow. Fig. 2 shows the normalized growth rate, $(s_1\eta)/E$, as a function of the normalized wave number, kh, for $\varepsilon_0 = -0.012$, $\nu = 0.3$, and various values of H/h, the thickness ratio between the viscous layer and the elastic film.

The critical wave number in Eq. (38) is a positive real number only when $\varepsilon_0 < 0$, i.e., when the film is initially compressed. In the other words, if the film is stress free ($\varepsilon_0 = 0$) or under tension ($\varepsilon_0 > 0$), both s_1- and s_2-modes decay and the flat film is stable. For a film under compression, the critical wave number is the result of the compromise between the energy reduction associated with in-plane expansion of the film and the energy addition associated with bending. At the critical wave number ($k = k_c$), the bending energy is in balance with the in-plane energy reduction, and the growth rate is zero ($s_1 = 0$). For perturbations with large wave number ($k > k_c$, short wavelength), the bending energy dominates and causes the perturbations to decay ($s_1 < 0$). For perturbations with small wave number ($k < k_c$, long wavelength), the reduction in the energy corresponding to compression overcomes the bending energy and drives the perturbations to grow

($s_1 > 0$). As the wave number approaches zero, the wavelength is so long that the driving force to grow the perturbations, the energy reduction associated with the growth, is very small, and meanwhile the viscous matter under the film has to be transported over a long distance for the perturbations to grow. Consequently, the growth rate approaches zero ($s_1 \to 0$) when $k \to 0$.

As shown in Fig. 2, the critical wave number is independent of the thickness ratio between the viscous layer and the elastic film. Actually, the critical wave number is the same as that for Euler buckling of a free-standing film subject to a compressive stress. Since the critical wave number is purely determined by the energetic of the expansion and bending of the elastic film, the viscous layer has no effect on the critical wave number. The flow of the viscous layer, however, sets the time scale for the growth of the unstable modes. The growth rate, s_1, is inversely proportional to the viscosity, η. For $k < k_c$, the normalized growth rate, $(s_1\eta)/E$, increases as the thickness ratio, H/h, increases, i.e., the thicker the viscous layer, the more readily it flows.

In the limit of an infinitely thick viscous layer ($H/h \to \infty$), the growth rate s_1 becomes

$$s_1 = \frac{Ekh}{24\eta(1-\nu^2)}(-12\varepsilon_0(1+\nu) - (kh)^2), \tag{39}$$

which is the same as that obtained in Sridhar et al. (2001). In the other limit, when the thickness of the viscous layer is small ($H/h \to 0$), the growth rate is

$$s_1 = \frac{Ekh(kH)^3}{144\eta(1-\nu^2)}(-12\varepsilon_0(1+\nu) - (kh)^2), \tag{40}$$

which is the same as that obtained in Huang and Suo (2002), but is only one-quarter of that obtained in Sridhar et al. (2001).

Since the growth rate is zero at the critical wave number and approaches to zero in the limit of zero wave number, there must exist a wave number in between that maximizes the growth rate. The fastest growing wave number, k_m, is found by setting $\partial s_1/\partial k = 0$. Fig. 3a shows the normalized fastest growing wave number, $k_m h$, as a function of the initial compressive strain, ε_0, for various thickness ratios, and Fig. 3b shows the normalized growth rate, $(s_m\eta)/E$, corresponding to k_m. Both the wave number and the growth rate increase as the compressive strain increases. As the thickness ratio increases, the fastest growing wave number decreases, but the corresponding growth rate increases.

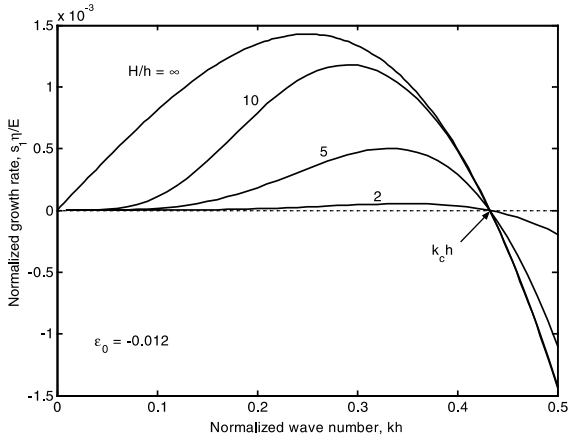

Fig. 2. Normalized growth rate of the linear perturbations vs the normalized wave number for various thickness ratios.

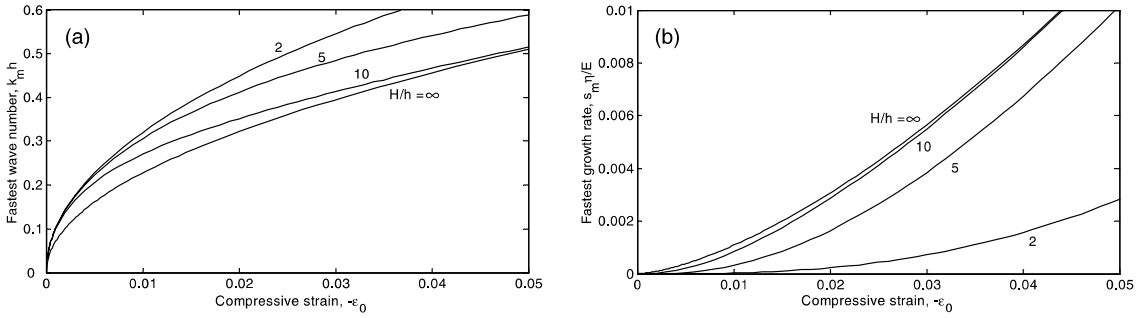

Fig. 3. The fastest growing wave number and the corresponding growth rate vs the compressive strain for various thickness ratios.

Fig. 4 compares the growth rate from the present study (solid lines) with the previous studies for two different thickness ratios. The dashed lines are the growth rate from Sridhar et al. (2001), and the dotted lines from Huang and Suo (2002). Both studies obtain the same critical wave number as in the present study, but the growth rates for the unstable modes are different. In Sridhar et al. (2001), the shear traction at the interface was assumed to be zero and the displacement parallel to the interface was ignored. As we discussed before, the analysis is approximately correct for a thick viscous layer. In Huang and Suo (2002), the lubrication theory was used and the thickness of the viscous layer was assumed to be small compared to the wavelength. The present study does not make assumptions about the thickness of the viscous layer. Fig. 4a shows that, for a thin viscous layer ($H/h = 2$), the result from Sridhar et al. (2001) is not good compared to the more rigorous result from the present study, but the result from Huang and Suo (2002) is better in agreement. The situation is reversed for a thick viscous layer, as shown in Fig. 4b for $H/h = 5$.

Fig. 5a shows the fastest growing wave number as a function of the thickness ratio for $\varepsilon_0 = -0.012$ and $v = 0.3$, and Fig. 5b shows the corresponding growth rate. The results from the previous studies are also plotted for comparisons. In the limit of an infinitely thick viscous layer ($H/h \to \infty$), the fastest growing wave number is

$$k_m h = \sqrt{-4\varepsilon_0(1+v)}, \tag{41}$$

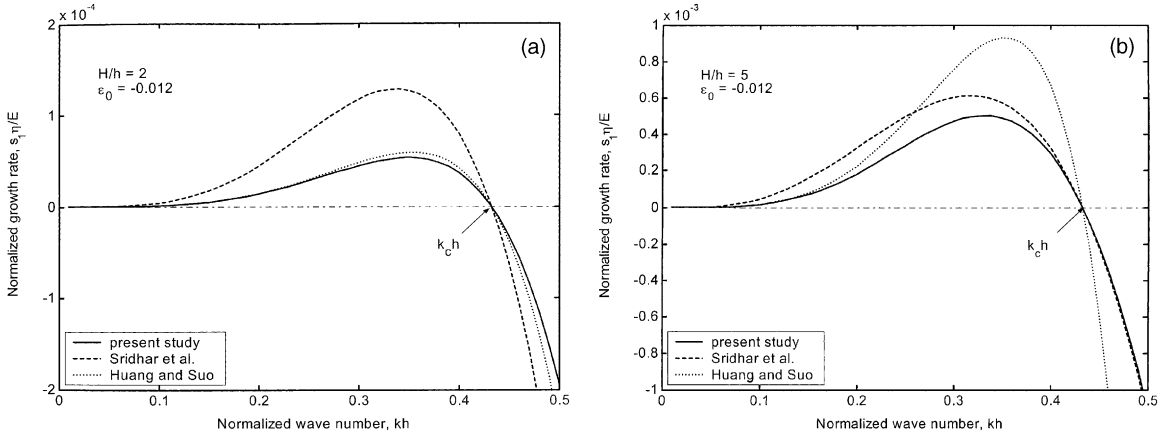

Fig. 4. Comparisons of the growth rate from the present study with those from the previous studies for two different thickness ratios: (a) $H/h = 2$; (b) $H/h = 5$.

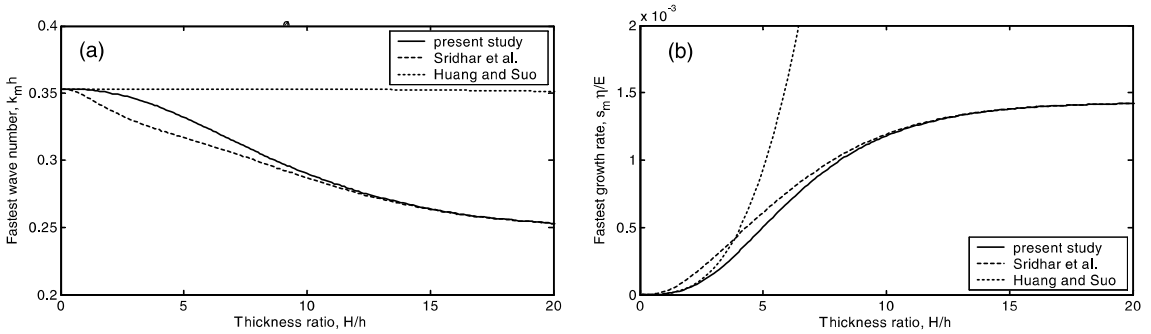

Fig. 5. Comparisons of the fastest growing wave number and the corresponding growth rate from the present study with those from the previous studies.

and the corresponding growth rate is

$$s_{\mathrm{m}} = \frac{E}{12\eta(1-v^2)}\left(-4\varepsilon_0(1+v)\right)^{3/2}. \tag{42}$$

As shown in Fig. 5, the result from Sridhar et al. (2001) agrees closely with the present study for large thickness ratios ($H/h > 10$) and is exactly the same in the limit of an infinitely thick viscous layer. For smaller thickness ratios, the agreement is poor. In the limit of small thickness ratio ($H/h \to 0$), the fastest growing wave number is

$$k_{\mathrm{m}}h = \sqrt{-8\varepsilon_0(1+v)}, \tag{43}$$

and the corresponding growth rate is

$$s_{\mathrm{m}} = \frac{16E}{9\eta(1-v^2)}\left(-\varepsilon_0(1+v)\frac{H}{h}\right)^3. \tag{44}$$

Eqs. (43) and (44) are the same as the results from Huang and Suo (2002). Fig. 5 shows that the agreement between the dotted line and the solid line is good for $H/h < 3$, but becomes increasingly poor for both the fastest wave number and the growth rate as the thickness ratio increases. In the same limit, $H/h \to 0$, the fastest growing wave number from Sridhar et al. (2001) approaches Eq. (43), but the corresponding growth rate is four times of Eq. (44). The difference between the solid line and the dashed line in Fig. 5b at small thickness ratio is not obvious because they both approach zero as $H/h \to 0$.

4. Concluding remarks

The stability of a flat, compressed elastic film on a viscous layer is studied by a linear perturbation analysis. The critical wave number is the same as that for Euler buckling of a free-standing film subject to a compressive stress. The viscous layer has no effect on the instability condition. The flow of the viscous layer only sets the time scale for the growth of the unstable modes. The fastest growing wave number and the corresponding growth rate are obtained as functions of the compressive strain and the thickness ratio between the elastic film and the viscous layer. Comparing to the previous studies, the present analysis is more rigorous in the sense that it does not make any assumptions about the thickness of the viscous layer and thus is valid for all thickness range. In the limits of infinitely thick ($H \to \infty$) and thin ($H \to 0$) viscous layer, the results from the present study reduce to those from the previous studies.

One must note that the result from the linear perturbation analysis in the present study is only valid for a short time. As the perturbation amplitude grows, the non-linear plate theory for large deflection has to be used, and some approximation of the flow in the viscous layer has to be made. Nevertheless, the growth rate from the linear perturbation analysis provides an estimate of the time scale for wrinkling, and the fastest growing wave number may be compared to the observed wave number in experiments. However, no effort has been made in the present study to compare with experiments, because the comparisons will only make senses with more details of experiments and other models, which will be presented elsewhere.

Acknowledgements

The work is supported by the National Science Foundation through grants CMS-9820713 and CMS-9988788 with Drs. Ken Chong and Jorn Larsen-Basse as the program directors. We thank J.H. Prevost, D.J. Srolovitz, N. Sridhar, J.C. Sturm, and H. Yin for helpful discussions.

Appendix A. Exact solution for two-dimensional flow in a viscous layer

The governing equations for the Stokes flow, Eqs. (1)–(4), are reduced by assuming a two-dimensional flow under the plane strain conditions, i.e., $v_x = v_x(x,z)$, $v_z = v_z(x,z)$, and $v_y = 0$. The equilibrium equation, Eq. (1), becomes

$$\frac{\partial \sigma_{xx}}{\partial x} + \frac{\partial \sigma_{xz}}{\partial z} = 0 \quad \text{and} \quad \frac{\partial \sigma_{xz}}{\partial x} + \frac{\partial \sigma_{zz}}{\partial z} = 0. \tag{A.1}$$

The stress components are

$$\sigma_{xx} = 2\eta \frac{\partial v_x}{\partial x} - p, \tag{A.2}$$

$$\sigma_{zz} = 2\eta \frac{\partial v_z}{\partial z} - p, \tag{A.3}$$

$$\sigma_{xz} = \eta \left(\frac{\partial v_x}{\partial z} + \frac{\partial v_z}{\partial x} \right), \tag{A.4}$$

and

$$p = -\tfrac{1}{2}(\sigma_{xx} + \sigma_{zz}). \tag{A.5}$$

The continuity equation, Eq. (3), becomes

$$\frac{\partial v_x}{\partial x} + \frac{\partial v_z}{\partial z} = 0. \tag{A.6}$$

The stresses and velocities can be represented by two potentials, $U(x,z)$ and $\chi(x,z)$, as below:

$$\sigma_{xx} = \frac{\partial^2 U}{\partial z^2}, \quad \sigma_{zz} = \frac{\partial^2 U}{\partial x^2}, \quad \sigma_{xz} = -\frac{\partial^2 U}{\partial x \partial z}, \tag{A.7}$$

$$v_x = \frac{1}{2\eta} \left(-\frac{\partial U}{\partial x} + 2\frac{\partial \chi}{\partial z} \right), \quad v_z = \frac{1}{2\eta} \left(-\frac{\partial U}{\partial z} + 2\frac{\partial \chi}{\partial x} \right). \tag{A.8}$$

The equilibrium equation, Eq. (A.1), is automatically satisfied by Eq. (A.7). Eqs. (A.2)–(A.6) are satisfied by requiring that

$$\frac{\partial^2 \chi}{\partial x^2} + \frac{\partial^2 \chi}{\partial z^2} = 0 \quad \text{and} \quad \frac{\partial^2 U}{\partial x^2} + \frac{\partial^2 U}{\partial z^2} = 4\frac{\partial^2 \chi}{\partial x \partial z}. \tag{A.9}$$

A set of exact solutions to the equations in (A.9) gives that

$$U = \frac{1}{k^2}(C_1\cosh(kz) + C_2\sinh(kz) + C_3 kz\cosh(kz) + C_4 kz\sinh(kz))\sin(kx), \tag{A.10}$$

$$\chi = -\frac{1}{2k^2}(C_3\cosh(kz) + C_4\sinh(kz))\cos(kx), \tag{A.11}$$

where k is the wave number and C_j $(j = 1,\ldots,4)$ are constants to be determined from boundary conditions. Thus, from Eqs. (A.7) and (A.8), the stress components and the velocities are

$$\sigma_{xx} = (C_1\cosh(kz) + C_2\sinh(kz) + C_3(2\sinh(kz) + kz\cosh(kz)) + C_4(2\cosh(kz) + kz\sinh(kz)))\sin(kx), \tag{A.12}$$

$$\sigma_{zz} = -(C_1\cosh(kz) + C_2\sinh(kz) + C_3 kz\cosh(kz) + C_4 kz\sinh(kz))\sin(kx), \tag{A.13}$$

$$\sigma_{xz} = -(C_1\sinh(kz) + C_2\cosh(kz) + C_3(\cosh(kz) + kz\sinh(kz)) + C_4(\sinh(kz) + kz\cosh(kz)))\cos(kx), \tag{A.14}$$

$$v_x = -\frac{1}{2\eta k}(C_1\cosh(kz) + C_2\sinh(kz) + C_3(\sinh(kz) + kz\cosh(kz)) + C_4(\cosh(kz) + kz\sinh(kz)))\cos(kx), \tag{A.15}$$

$$v_z = -\frac{1}{2\eta k}(C_1\sinh(kz) + C_2\cosh(kz) + C_3 kz\sinh(kz) + C_4 kz\cosh(kz))\sin(kx). \tag{A.16}$$

For a viscous layer as shown in Fig. 1, the boundary conditions are specified at the bottom $(z = 0)$ and the surface $(z = H)$ of the layer. We assume no slip at the bottom of the viscous layer and set the velocities there to be zero, i.e.,

$$v_x(z = 0) = v_z(z = 0) = 0. \tag{A.17}$$

At the surface of the viscous layer, the normal and shear tractions take the form

$$\sigma_{zz}(z = H) = q_0\sin(kx), \tag{A.18}$$

$$\sigma_{zx}(z = H) = \tau_0\cos(kx). \tag{A.19}$$

By applying the boundary conditions, Eqs. (A.17)–(A.19), we obtain

$$C_1 = -C_4 = -\frac{\cosh(kH) + kH\sinh(kH)}{(kH)^2 + \cosh^2(kH)}q_0 + \frac{kH\cosh(kH)}{(kH)^2 + \cosh^2(kH)}\tau_0, \tag{A.20}$$

$$C_3 = -\frac{kH\cosh(kH)}{(kH)^2 + \cosh^2(kH)}q_0 - \frac{\cosh(kH) - kH\sinh(kH)}{(kH)^2 + \cosh^2(kH)}\tau_0, \tag{A.21}$$

and $C_2 = 0$.

Substituting Eqs. (A.20) and (A.21) into Eqs. (A.15) and (A.16), we obtain the velocities at the surface of the viscous layer as

$$v_x(z = H) = \frac{1}{2\eta k}\left(\frac{(kH)^2}{(kH)^2 + \cosh^2(kH)}q_0 + \frac{1}{2}\frac{2kH + \sinh(2kH)}{(kH)^2 + \cosh^2(kH)}\tau_0\right)\cos(kx), \tag{A.22}$$

$$v_z(z=H)=\frac{1}{2\eta k}\left(\frac{1}{2}\frac{\sinh(2kH)-2kH}{(kH)^2+\cosh^2(kH)}q_0+\frac{(kH)^2}{(kH)^2+\cosh^2(kH)}\tau_0\right)\sin(kx). \tag{A.23}$$

Note that the above solution is only exact for linear perturbation analysis of a viscous layer with a flat surface. For a viscous layer with a curved surface, the curvature of the surface has to be considered when specifying the boundary conditions.

References

Bowden, N., Brittain, S., Evans, A.G., Hutchinson, J.W., Whitesides, G.M., 1998. Spontaneous formation of ordered structures in thin films of metals supported on an elastomeric polymer. Nature 393, 146–149.

Evans, A.G., Hutchinson, J.W., 1984. On the mechanics of delamination and spalling in compressed films. International Journal of Solids and Structures 20, 455–466.

Evans, A.G., Mumm, D.R., Hutchinson, J.W., Meier, G.H., Pettit, F.S., 2001. Mechanisms controlling the durability of thermal barrier coatings. Progress in Materials Science 46 (5), 505–553.

Finot, M., Suresh, S., 1996. Small and large deformation of thick and thin-film multi-layers: effects of layer geometry, plasticity and compositional gradients. Journal of the Mechanics and Physics of Solids 44 (5), 683–721.

Freund, L.B., Nix, W.D., unpublished.

Hobart, K.D., Kub, F.J., Fatemi, M., Twigg, M.E., Thompson, P.E., Kuan, T.S., Inoki, C.K., 2000. Compliant substrates: a comprehensive study of the relaxation mechanisms of strained films bonded to high and low viscosity oxides. Journal of Electronic Materials 29 (7), 897–900.

Huang, R., Suo, Z., 2002. Wrinkling of an elastic film on a viscous layer. Journal of Applied Physics, 91, 1135–1142. Preprint available online at www.princeton.edu/~suo, Publication 120.

Huck, W.T.S., Bowden, N., Onck, P., Pardoen, T., Hutchinson, J.W., Whitesides, G.M., 2000. Ordering of spontaneously formed buckles on planar surfaces. Langmuir 16, 3497–3501.

Hutchinson, J.W., Suo, Z., 1992. Mixed mode cracking in layered materials. Advances in Applied Mechanics 29, 63–191.

Mumm, D.R., Evans, A.G., Spitsberg, I.T., 2001. Characterization of a cyclic displacement instability for a thermally grown oxide in a thermal barrier system. Acta Materialia 49 (12), 2329–2340.

Sridhar, N., Srolovitz, D.J., Suo, Z., 2001. Kinetics of buckling of a compressed film on a viscous substrate. Applied Physics Letters 78 (17), 2482–2484.

Suo, Z., 1995. Wrinkling of the oxide scale on an aluminum-containing alloy at high temperatures. Journal of the Mechanics and Physics of Solids 43 (6), 829–846.

Timoshenko, S., Woinowsky-Krieger, S., 1987. Theory of plates and shells, second ed. McGraw-Hill Inc., New York, pp. 378–380.

Tolpygo, V.K., Clarke, D.R., 1998a. Wrinkling of α-aluminum films grown by thermal oxidation—I. Quantitative studies on single crystals of Fe–Cr–Al alloy. Acta Materialia 46 (14), 5153–5166.

Tolpygo, V.K., Clarke, D.R., 1998b. Wrinkling of α-aluminum films grown by thermal oxidation—II. Oxide separation and failure. Acta Materialia 46 (14), 5167–5174.

Yin, H., Sturm, J.C., Suo, Z., Huang, R., Hobart, K.D., 2001. Modeling of in-plane expansion and buckling of SiGe islands on BPSG. Presented at the 43rd Electronic Materials Conference, Notre Dame, Indiana, June 2001, unpublished.